

ACOUSTOELECTRIC PROPERTIES OF GRAPHENE UNDER THE INFLUENCE OF SAW AND EXTERNAL ELECTRIC FIELD

Zinetula A. Insepov, Kurbangali B. Tynyshtykbayev

Nazarbayev University, NURIS, www.nu.edu.kz

Kabanbay Batyr str., 53, 010000 Astana, Kazakhstan

ktynyshtykbayev@nu.edu.kz, kt011@mail.ru

Oleg V. Kononenko, Dmitry V. Roshchupkin

Institute of Microelectronics Technology and High Purity Materials, Russian Academy of Sciences, http://www.ipmt-hpm.ac.ru

Akad. Osip'yan str., 6, 142432 Moscow, Chernogolovka, Russian Federation

dmitry.roshchupkin@iptm.ru

Abstract. The effect of SAW on the electrical properties of the few-layer (2-3 layers) graphene is studied. Under the influence of SAW the appearance of acoustoelectric current I_{AEC} in graphene is observed. The sign and magnitude of the induced I_{AEC} in graphene conditioned by magnitude and direction of the electromagnetic fields induced by SAW and an external electric field. When the direction of SAW and V_{bias} is the same I_{AEC} amplified, when at the opposite direction $-I_{AEC}$ are reduced in result of the interaction of these fields with each other. As a result of the measurement of the induced acoustoelectric (I_{AEC}) current in graphene under the influence of a surface acoustic wave (SAW) the fluctuation nature of acoustoelectric current in the area of electrical neutrality is established at low voltages of an external bias (V_{bias}) applied on a graphene. The fluctuation character of the I_{AEC} is manifested in all cases of measurements depending on the action of SAW and V_{bias} near the point of electrical neutrality. Chaotic fluctuation potential of graphene in the area of electrical neutrality is enhanced by the action of SAW that allows observing it in real conditions of the experiment at room temperature in air. The magnitude of I_{AEC} depends on the power of SAW, while there is a parabolic dependence of the induced I_{AEC} on the amplification current of SAW power (I_{SAW}). The parabolic dependence of I_{AEC} on I_{SAW} explained by specific relaxation of acoustic phonons of the piezocrystallic substrate, which is dominant in the process of electron-phonon scattering in graphene and acoustoelectric current induction in it. For large magnitudes of V_{bias} strict linear dependence of the I_{AEC} on V_{bias} is observed. Large V_{bias} effectively suppress the appearance of the fluctuation potential of electrons and holes. The ability to control the magnitude and direction of I_{AEC} induced in graphene by SAW is of practical importance.

Keywords: graphene, surface acoustic wave, voltage bias, acoustoelectric current, SAW-device

PACS: 85.05.ue

Bibliography – 14 references

Received 14.09.2015

RENSIT, 2015, 7(2):153-161

DOI: 10.17725/rensit.2015.07.153

CONTENS

1. INTRODUCTION (153)
 2. EXPERIMENTAL METHODS (154)
 3. RESULTS (155)
 4. DISCUSSIONS (156)
 5. CONCLUSIONS (158)
- REFERENCES (159)

1. INTRODUCTION

The unique electronic properties of graphene [1] can be controlled not only by an electric field [2, 3] but also by the surface acoustic wave [4, 5]. It is shown the possibility of generating acous-toelectric current in graphene under the influence of SAW [4], and the effect of amplification of the surface acoustic wave

(SAW) on the surface of the piezoelectric crystal $\text{La}_3\text{Ga}_5\text{SiO}_{14}$ upon application of an external electric voltage bias on the graphene lying between two high frequency signal interdigital transducers is detected [5]. SAW amplification takes place when direction of an external electric field was identical to the direction of SAW propagation on the surface of a piezoelectric crystal, in conductive graphene film, which is in contact with the surface of the piezoelectric crystal generating SAW, an electric current flow induces acoustoelectric current in the piezoelectric crystal that appears to enhance the amplitude of the SAW.

The effect of the SAW amplitude amplification in graphene coated SAW-structures is observed upon application of small electric field to the graphene that opens up new possibilities for creating a contactless acoustooptical and acoustoelectric devices based on graphene. All this cause great interest to study the interaction of SAW with graphene.

In this study, we investigate the effect of SAW on the nature acoustoelectric current appearance in graphene by applying an external electric field, depending on the amplitude and direction of it.

2. EXPERIMENTAL METHODS

In the experiment, coated with graphene $\text{La}_3\text{Ga}_5\text{SiO}_{14}$ (LGS), LiNbO_3 Y-cut piezocrystals samples are used as SAW substrate. These crystals, like a quartz SiO_2 , possess point group symmetry 32 but unlike SiO_2 have the high values of piezoelectric constants and electromechanical coupling coefficients. Substrates from Y-cut the crystal (planes (100) parallel to the crystal surface) were used to fabricate the SAW devices. On the crystal surface to excite the SAW the interdigital transducer (IDT) was fabricated

by photolithography. The IDT consisted of 50 pairs of electrodes. On the Y-cut of the LGS crystal the IDTs were fabricated to excite the SAW with the wavelength $\Lambda = 30 \mu\text{m}$ at the resonance excitation frequency $f = 75.33$ MHz which propagates with the velocity $V = f \times \Lambda = 2260$ m/s along the X axis. The IDT on the Y-cut of the LiNbO_3 crystal excites the SAW with the wavelength $\Lambda = 4 \mu\text{m}$ at the resonance excitation frequency $f = 860$ MHz which propagates at $V = 3440$ m/s along the X axis.

The graphene film on the piezoelectric substrate surface was formed between two IDTs by the transfer method [6]. Ni film was deposited by the ion sputtering deposition technique on the surface of an oxidized Si(100). The target was high purity Ni (99.9999%). Ion sputtering was performed in vacuum of 10^{-6} Torr. The sputtered film thickness of Ni was $\sim 0.3 \mu\text{m}$. Then the substrate with the sputtered Ni film was placed into a quartz reactor tube pumped down to a pressure about 10^{-6} Torr and then inserted into a furnace preheated to 950°C . When the samples were heated to the reaction temperature, acetylene was let into the quartz tube up to a pressure of 0.4 Torr for 5 s and then pumped out and the quartz tube reactor was extracted from the furnace. Transfer of the resulting graphene was done with the aid of polymethylmethacrylate (PMMA) that was spin coated onto the surface of the graphene film to serve as a support. The PMMA/graphene layer was detached from the substrate by wet-etching of the Ni film with a 1% water solution of hydrochloric acid and then manually laid on the piezoelectric substrate between two IDTs. PMMA was then removed from the graphene surface by exposure to acetone in vapor and then in liquid form.

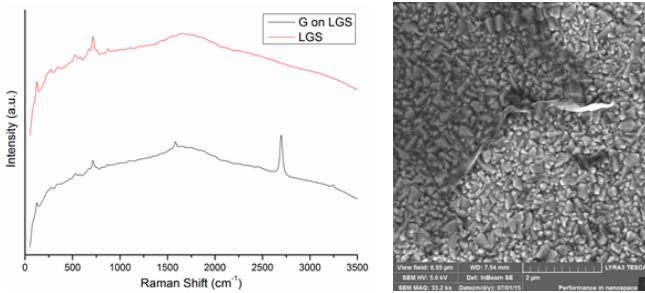


Fig. 1. Raman spectra of LGS-substrate (red) and graphene on LGS-substrate (black) shown the characteristic D-, G-, and 2D-peaks. The ratio $I_{2D}/I_G \approx 2$ indicates that the graphene film consists of (2–3) layers of graphene (FLG).

Quality control of the graphene was carried out using a Raman microscope SENTERRA (Bruker) at wavelengths of laser excitation 488 nm, 532 nm and 735 nm.

Fig. 1 shows Raman spectra of LGS piezoelectric substrate and graphene measured its transfer onto the LGS piezoelectric substrate, and electron microscopic images of graphene were obtained by scanning electron microscope LYRA 3, TESCAN. The Raman spectra were registered using the blue laser with the 488 nm wavelength at SENTERRA Raman microscope. The ratio of intensities of two peaks $I_{2D}/I_G = 2$ shows that the graphene film has of 1÷3 layers. To study the electric properties of graphene under the conditions of SAW propagation, two Al electrodes were formed on the graphene film surface by electron beam lithography. The distance between two electrodes was ~ 3 mm. **Fig. 2** shows the SAW devices with graphene which were used to investigate the influence of

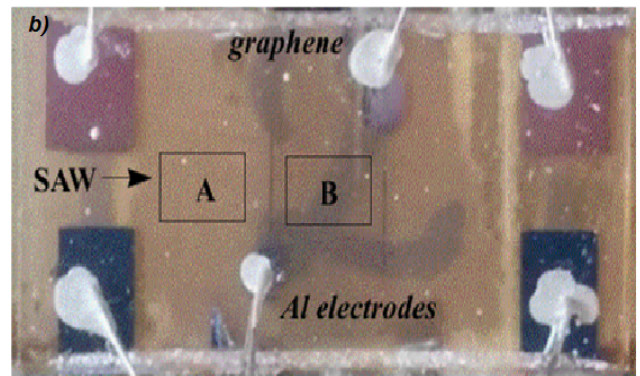
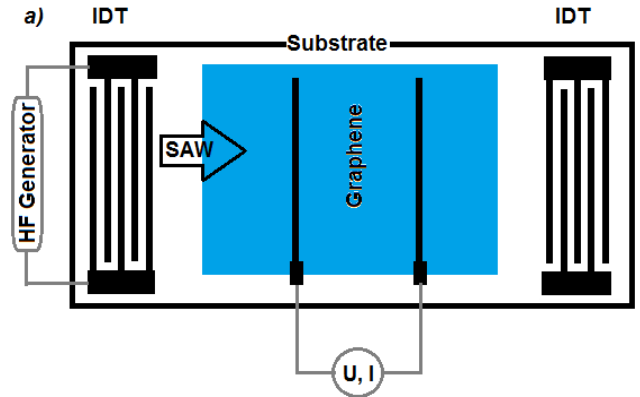


Fig. 2. Circuit (a) and photo (b) of SAW device.

SAW propagation on the electrical properties of graphene.

Generation and registration of SAW signal and graphene acoustoelectric current I_{AEC} were performed by using a high-frequency generator APH-2140 and KEITHLEY 2400 Source Meter according to the circuit diagram in Fig. 2a.

3. RESULTS

Fig. 3 shows the current-voltage characteristics dependence of I_{gr} and I_{AEC} currents through graphene on the applied bias voltage V_{bias} of an external electric field in the absence of SAW (Fig. 3a, $I_{gr} f(V_{bias})$), and under the

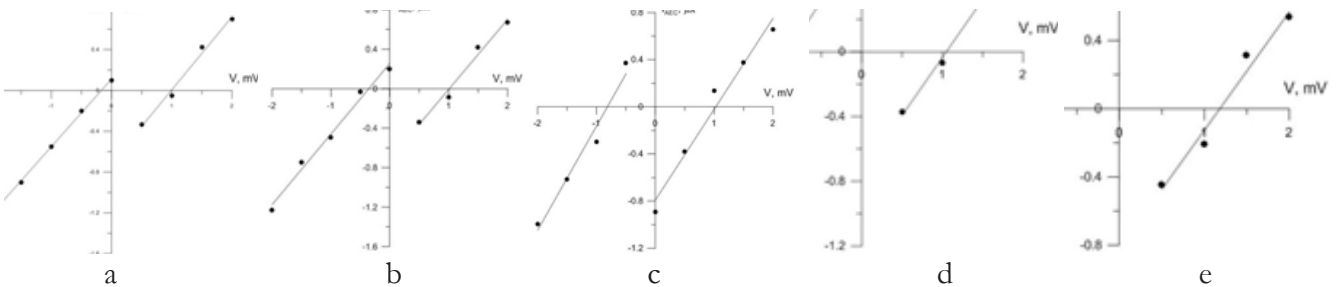


Fig. 3. Dependences of acoustoelectric current through the graphene I_{AEC} from an external electric field bias V_{bias} under the influence of a SAW with a frequency $f = 54.2$ MHz at various currents gain SAW I_{saw} : a) $I_{saw} = 0$ mA; b) $I_{saw} = 25$ mA; c) $I_{saw} = 50$ mA; d) $I_{saw} = 75$ mA; e) $I_{saw} = 100$ mA. Power of source SAW IDT $W = 1.07$ Wt.

influence of SAW on the graphene (Fig. 3b-3e, $I_{AEC} f(V_{bias})$). I_{gr} – current through the graphene in the absence of SAW, I_{AEC} -induced acoustoelectric current through the graphene at different amplification currents I_{saw} of SAW power.

However, for small bias voltage V_{bias} (near $V_{bias} \approx 0$) it fails to measure the magnitude of current through the graphene because of the large fluctuations of its magnitude due to large measurement errors.

It should be noted that in all cases, the measurement of $I_{gr} f(V_{bias})$ and $I_{AEC} f(V_{bias})$ dependences do not pass through the point of electrical neutrality (0) in the absence of an external electric field, $V_{bias} = 0$. This area is shown as the decoupling dependences of $I_{gr} f(V_{bias})$, Fig. 3a and $I_{AEC} f(V_{bias})$, Fig. 3b-3e.

A more detailed analysis shows that in the low-voltage $V_{bias} \sim 0$ near the point of electrical neutrality [1], there is an interesting feature of the changes in the magnitude and sign of acousto-electric current I_{AEC} charge carriers in graphene under the influence of SAW, the magnitude and direction of the applied external electric field bias potential V_{bias} .

Close to the $V_{bias} \sim 0$, for both positive ($V_{bias} > 0$) and negative ($V_{bias} < 0$) bias voltages there is a change of sign of the current I_{gr} through the graphene and decoupling dependence $I_{gr} f(V_{bias})$, Fig. 3a.

When the SAW turned on the magnitude of the decoupling of $I_{AEC} f(V_{bias})$ dependence near $V_{bias} \sim 0$ increases (Fig. 3b). With increasing current amplification I_{saw} SAW power that gap even more greater (Fig. 3b-3e). With increasing current amplification I_{saw} SAW power change of acoustoelectric current I_{AEC} the sign is observed for large values of negative-bias voltage ($V_{bias} < 0$). For positive values of the bias voltage ($V_{bias} > 0$) change of current I_{gr} sign for SAW of various power takes place almost at the same value of V_{bias}

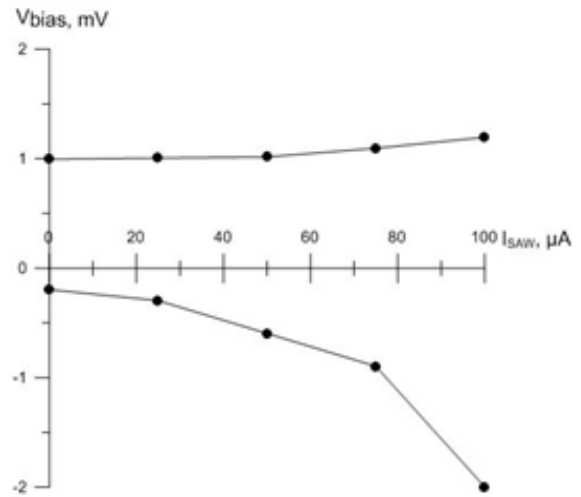


Fig. 4. The dependences of V_{bias} from I_{saw} , at which the sign change acoustic electrical current I_{AEC} = 1.0 mV (Fig. 3). The dependence V_{bias} on the current amplification I_{saw} of SAW power becomes quadratic when there is a change in the sign I_{AEC} (Fig. 4).

Fig. 5 shows the dependence of the I_{AEC} acoustoelectric current on amplification current I_{saw} of SAW power at different values and signs of V_{bias} . Magnitude of I_{AEC} , arising under the influence of SAW, increases when a negative bias voltage $V_{bias} < 0$ (Fig. 5) applied and decreases with the positive $V_{bias} > 0$ (Fig. 5b). The dependence of the I_{AEC} on amplification current I_{saw} of SAW power is quadratic in nature (Fig. 5).

At high bias voltages V_{bias} strict linear dependence of the I_{AEC} on applied voltage (Fig.

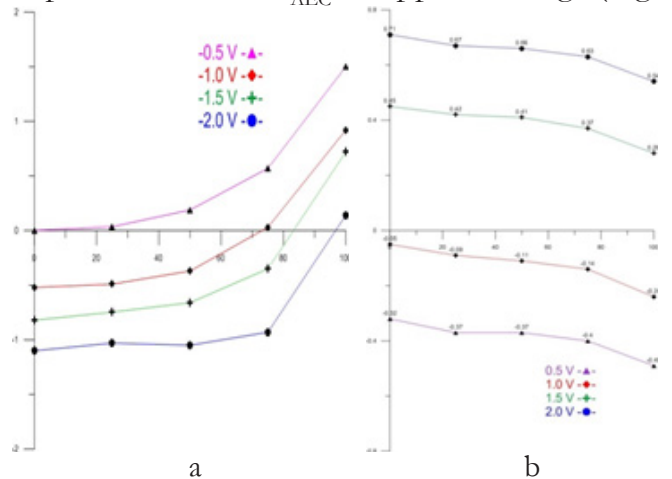


Fig. 5. Dependences of acoustoelectric current (I_{AEC}) from the current power amplifier SAW (I_{saw}) at negative ($V_{bias} < 0$) (a) and positive ($V_{bias} > 0$) (b) values of the bias voltage.

3) is observed. With these values V_{bias} applied external electric field effectively suppress the occurrence of fluctuation potential [7] and in graphene common characteristic of the traditional con-ductors dependence of the current of the ohmic contact on voltage is realized.

4. DISCUSSIONS

It is known [3 - 5] that under the influence of SAW acoustoelectric current I_{AEC} is induced in graphene. The magnitude of the induced I_{AEC} increases linearly with SAW power [3]. When an additional external bias voltage of the electric potential applied on the graphene value of the I_{AEC} depends on the direction of the applied electric field [5] and increases when SAW propagation direction and an external electric field are the same, and decreases if they are in the opposite direction (Fig. 3).

Acoustoelectric current I_{AEC} was measured according to the scheme applying of positive voltage to the graphene electrodes in the direction of propagation of SAW (Fig. 2). The electron current flows from the left electrode to the right, changing the polarity - on the contrary, from right to left. The direction of the SAW remains constant – from the left IDT source of SAW to the right IDT. When the direction of SAW propagation direction and the external electric field (negative voltage $V_{\text{bias}} < 0$) are the same I_{AEC} is amplified, otherwise – inhibited. This is manifested in the form of a quadratic dependence of acoustoelectric current I_{AEC} on current amplification I_{saw} of SAW power in the case of coincidence of directions of SAW propagation and of external electric field with a negative bias voltage $V_{\text{bias}} < 0$. In the case of opposite directions of SAW and $V_{\text{bias}} > 0$ I_{AEC} decreases, despite the increase SAW power, increasing I_{saw} .

I_{AEC} decoupling at the low bias voltages V_{bias} (near $V_{\text{bias}} \sim 0$) and the change a sign of the charge carriers (Fig. 3), we tend to explain by peculiar features of the electronic properties of graphene near the point of electrical neutrality under the influence of a SAW.

According to [1, 2, 7], the point of electrical neutrality in graphene (note, with the high mobility of charge carriers), the area near which by an equal concentration of the offsetting each other electrons and holes [1] or zero carrier concentration (or on the approach to it [2]), a sharp increase in the resistance of the sample is observed [7].

In the real condition there is always a chaotic fluctuation potential in graphene, due to the two-dimensional nanowave crystal structure and thermal fluctuations, which disappear only at $T = 0$ K [2, 7]. Raising or lowering the local potential leads to the fact that the two-dimensional electron gas is broken down into "puddles" of electrons and holes [2]. And it manifests itself at low carrier concentrations when there is no overlap of fluctuating fields. That is, graphene has amphoteric (ambipolar), conductivity, presence of two types of charges – electrons and holes, at the negative voltage type of electronic type prevails, with a positive voltage positive charges are become dominating. Near the field of electrical neutrality a mutual cancellation of the charge carriers takes place. Near electroneutrality point both types of charges that cancel each other are presented, thus cause the electric potential fluctuation of graphene [2].

In our case, the fluctuation character of acoustoelectric current through the graphene near a small electrical voltage due to the influence of the alternating electric field of the piezoelectric crystal, accompanied by the generation and distribution of SAW which leading to the elastic deformation of graphene/piezocrystal [9]. SAW causing

elastic deformation of the surface layer of the piezoelectric induces electric polarization that leads to an alternating electric field of SAW, both inside and outside of the piezoelectric crystal, which is reflected in the fluctuations of Dirac fermions in graphene [8] and changing the sign of the electric current in graphene [9].

Deformation amplitude of the surface layer of piezoelectric crystal, determined by using the high-resolution X-ray diffraction method on a synchrotron radiation source BESSY II, can be changed depending on the power of SAW.

In conditions of this experiment, the deformation amplitude of graphene changes within range $h = 0 - 1.8 \text{ \AA}$, depending on the changes of applied on IDT the high-frequency signal amplitude $U = 0 - 25 \text{ V}$ and with period $\Lambda = 30 \text{ microns}$ with SAW frequency $f = 75.33 \text{ MHz}$ for LGS-substrates [9]. The deformation of graphene results in fluctuations of its electric field in areas of local increase or decrease of the electric potential of two-dimensional electron gas is broken down into "puddles" of electrons and holes, respectively [2], which are spatially separated by a period equal to $\Lambda_{\text{SAW}} = 30 \text{ microns}$ (LGS). This is manifested in the form of decoupling $I_{\text{AEC}} f(V_{\text{bias}})$ and change the sign of the charge carriers at low voltages (Fig. 3-5). With an increase of amplification current I_{SAW} of SAW power the sign change of I_{AEC} is observed for high negative bias voltages $V_{\text{bias}} < 0$. Thus, with the increase of the amplitude of the SAW power there is a trend of sign changing in the I_{AEC} with increasing value of the negative bias voltage $V_{\text{bias}} \approx -0.2 \text{ mV}$ up $V_{\text{bias}} \approx -1.0 \text{ mV}$ (Fig. 3, 4). While the sign change of I_{AEC} when a positive bias voltage $V_{\text{bias}} > 0$ applied occurs at a constant value of V_{bias} , about 1.0 mV irrespective SAW power (Fig. 3 and 4).

When an external electric field applied on the graphene, and under the influence of SAW at low bias voltages V_{bias} the sign change of I_{AEC} is observed depending on the amplification current I_{SAW} of SAW power (Fig. 3-5). With an increase of amplification current I_{SAW} of SAW power the sign change of I_{AEC} is observed for high negative bias voltages $V_{\text{bias}} < 0$. Thus, with the increase of the amplitude of the SAW power there is a trend of sign changing in the I_{AEC} with increasing value of the negative bias voltage $V_{\text{bias}} \approx -0.2 \text{ mV}$ up $V_{\text{bias}} \approx -1.0 \text{ mV}$ (Fig. 3, 4). While the sign change of I_{AEC} when a positive bias voltage $V_{\text{bias}} > 0$ applied occurs at a constant value of V_{bias} , about 1.0 mV irrespective SAW power (Fig. 3 and 4).

At high bias voltages V_{bias} strict linear dependence of the I_{AEC} on applied voltage (Fig. 3) is observed. At these values of V_{bias} applied external electric field effectively suppress the occurrence of potential fluctuation [7].

It should be noted the distinctive feature of the fluctuating nature of the manifestation acoustoelectric current through the graphene near the small voltages in our experiment from the experimental conditions [1, 2, 7], when monolayer or double-layer graphene obtained by micromechanical cleavage highly oriented pyrolytic graphite (HOPG) is used. Wherein graphene films are suspended between the metal contacts on the substrate of oxidized silicon [1, 2] or encapsulated in thin layers of boron nitride crystallite obtained by micromechanical cleavage from boron nitride crystal [7]. The mobility of the charge carriers in graphene samples were about $10^6 \text{ cm}^2\text{V}^{-1}\text{s}^{-1}$ for suspended graphene and $10^5 \text{ cm}^2\text{V}^{-1}\text{s}^{-1}$ for encapsulated graphene. Measurements are performed at low temperatures, 4 K , 20 K , in an inert environment. In our case, 2-3 layer graphene was used synthesized by chemical vapor

deposition by using acetylene vapor-grown "in situ" Ni-catalysts. Mobility was equal to $4800 \text{ cm}^2\text{V}^{-1}\text{s}^{-1}$ [5]. And this graphene film is placed between IDT on a piezoelectric substrate of lithium niobate crystals LiNbO_3 and langasite $\text{La}_3\text{Ga}_5\text{SiO}_{14}$. Measurements are performed in air at room temperature.

Nevertheless, the effect of SAW on the graphene leads to additional conditions for the manifestations of fluctuations of charge carriers in graphene, which is observed in our experiment at ambient temperature in air.

The parabolic dependence of acoustoelectric current I_{AEC} through graphene which depends on the amplification current I_{SAW} of SAW power and an external electric field at the coincidence of their directions (Fig. 5a) can be explained as follows. SAW on the graphene gives rise to a acoustoelectric current due to the interaction of electromagnetic fields SAW and an electric current through the graphene by applying an electrical bias voltage. As a result, the electron-phonon scattering, which is large in graphene [1], part of the energy is lost to this SAW. Energy relaxation of acoustic phonons of graphene depends on the temperature of the crystal lattice [10 -12].

In graphene relaxation time of acoustic phonons inversely proportional to the square of the temperature T_e

$$t_{\text{relax}}(\text{Graphene}) \sim T_e^{-2},$$

while for acoustic phonon relaxation time of piezocrystal substrate (t_{relax}) at high temperatures have a linear dependence on T_e and does not depend on the degree of degeneracy of the electron gas [13]

$$t_{\text{relax}}(\text{SAW}) \sim T_e^{-1}.$$

In addition it is necessary to consider that any external disturbance on two or more layer graphene has effects not only on existing carriers, but also creates additional carriers [1, 2, 6, 14].

It should be noted, that this electron-phonon relaxation process in the graphene may be controlled by an external piezoelectric coupling and an external electric field.

Thus, the results of this work show possibility to control acoustoelectric current in graphene by external SAW and electric fields. These features, along with the possibility of amplification the SAW amplitude [4], and controlling the amount and direction of the current in graphene on the surface of the piezoelectric crystals by changing the amplitude of SAW are of practical interest for the future development of various devices based on graphene, such as solar panels with nanoantennas in the terahertz range, nanopumps and fuel cells, two-dimensional nanomembranes etc.

4. CONCLUSIONS

1. The effect of SAW on the electrical properties of the few-layer (2-3 layers) graphene is studied. Acoustoelectric current I_{AEC} amplification in graphene under the influence of SAW is observed. The sign and magnitude of I_{AEC} depends on the magnitude and direction of SAW and an external electric field, V_{bias} . At the same direction of SAW and V_{bias} the amplification of process of inducing I_{AEC} is observed, at the opposite direction – the braking of process of inducing I_{AEC} is observed.
2. Results of the I_{AEC} measurements induced in graphene under influence of SAW establish the specific fluctuation of acoustoelectric current near the point of electrical neutrality, at low voltages of external bias, V_{bias} . The fluctuation nature of the I_{AEC} is manifested in all cases of measurements depending on the action of SAW and V_{bias} that allows observing in real conditions of the experiment at room temperature in air.

3. The value I_{AEC} depends on the SAW power, $t_{relax}(\text{Graphene}) \sim T_c^{-2}$. There is a parabolic dependence of I_{AEC} on I_{saw} . The parabolic dependence of the $I_{AEC} f(I_{saw})$ explained by mechanism of the relaxation of acoustic phonons of piezocrystal substrate, which is dominant in the process of electron-phonon scattering in graphene and inducing of acoustoelectric current in it.
4. At larger values of V_{bias} strict linear dependence of the I_{AEC} on V_{bias} is observed. Larger V_{bias} effectively suppresses the occurrence of fluctuation potential of electrons and holes.

The ability to control the magnitude and direction of I_{AEC} induced in graphene by SAW is of practical importance.

ACKNOWLEDGMENTS

The authors thank A.A. Ainabayev (Nazarbayev University) and A.V. Irzhak (IMTRAS) for help with the experiments and the processing of the results, M.V. Lukashova (LLC "TESCAN", St. Petersburg) for electron microscope images of graphene.

This work was funded by the Ministry of Education and Science of the Russian Federation (contract № 14.607.21.0047, registration number № RFMEFI60714X0047) and the Ministry of Education and Science of the Republic of Kazakhstan (contract № 265-12.02.2015). D.R. would like to thank the Russian Fund of Basic Researches (grant №14-02-91700) and Z.I. – Nazarbayev University Fund on the program "Stars of world science", anchor project № 031-2013).

REFERENCES

1. Geim AK, Novoselov KS. The rise of graphene. *Nature Materials*, 2007, 6:183-191; doi:10.1038/nmat1849.
2. Novoselov KS, Geim AK, Morozov SV, Jiang D, Zhang Y, Dubonos SV, Grigorieva IV, Firsov AA. Electric Field Effect in Atomically Thin Carbon Films. *Science*, 2004, 306:666-669.
3. Morozov SV. New effects in graphene with high carrier mobility. *Phys. Usp.*, 2012, 182(4):438-442.
4. Miseikis V, Cunningham JE, Saeed K, O'Rourke R, Davies AG. Acoustically induced current flow in graphene. *Appl. Phys. Lett.*, 2012, 100(133105):1-4.
5. Insepov Z, Emelin E, Kononenko O, Roshchupkin DV, Tynyshtykbayev KB, Baigarin KA. Surface acoustic wave amplification by direct current-voltage supplied to graphene film. *Applied Physics Letters*, 2015, 106 (023505):1-5; doi: 10.1063/1.4906033.
6. Matveev VN, Kononenko OV, Levashov VI, Volkov VT, and Kapitanova OO. Method of fabrication of graphene film. *Patent Russian Federation No. 2500616* (10 December 2013).
7. Morozov SV, Novoselov KS, Geim AK. Electron transport in graphene. *Phys. Usp.*, 2008, 178(7):776-780.
8. Thalmeier P, Dora B, Ziegler K. Surface acoustic wave propagation in graphene. *Phys. Rev. B*, 2010, 81(041409 (R)):1-4; arXiv:0909.0130.
9. Dmitry Roshchupkin, Luc Ortega, Ivo Zizak, Olga Ploticyna, Viktor Matveev, Oleg Kononenko, Evgenii Emelin, Alexei Erko, Kurbandali Tynyshtykbayev, Dmitry Irzhak, Zinetula Insepov. Surface acoustic wave propagation in graphene film. *JAP*, 2015, 118, in press. DOI: 10.1063/1.4930050.
10. Morozov SV, Novoselov KS, Katsnelson MI, Schedin F, Elias DC, Jaszczak JA, Geim AK. Giant Intrinsic Carrier Mobilities in Graphene and Bilayer. *Phys.Rev.Lett.*, 2008, 100(016602).
11. Chen JH, Jang C, Xiao S, Ishigami M, Fuhrer MS. Intrinsic and Extrinsic Performance

- Limits of Graphene Devices on SiO₂.
Nature Nanotech., 2008, 3:206.
12. Das Sarma S, Adam S, Hwang EH, Rossi E. Electronic transport in two-dimensional graphene. *Rev.Modern Phys.*, 2011, 83:407-470.
 13. Zhang SH, Xu W, Peeters FM, Badalyan SM. Electron energy and temperature relaxation in graphene on a piezoelectric substrate. *Phys.Rev.B*, 2014, 89(1954090):1-6; arXiv:1312.638v2.
 14. Lozovik YE, Merkulov SP, Sokolik AA. Quantum electron phenomena in graphene. *Phys. Usp.*, 2008, 178(7):757-776.